Thin-Walled Structures 80 (2014) 217–230

Contents lists available at ScienceDirect

Thin-Walled Structures

journal homepage: www.elsevier.com/locate/tws

Hysteretic behaviors of cold-formed steel beam-columns with hollow rectangular section: Experimental and numerical simulations

Na Yang [a,*], Ya'nan Zhong [a], Qing'tong Meng [a], Hao Zhang [b]

[a] School of Civil Engineering, Beijing Jiaotong University, Beijing 100044, China
[b] School of Civil Engineering, The University of Sydney, Sydney, NSW 2006, Australia

A R T I C L E I N F O

Article history:
Received 16 August 2013
Received in revised form
25 February 2014
Accepted 6 March 2014
Available online 17 April 2014

Keywords:
Local buckling
Cyclic loading
Cold-formed steel member with hollow section
Ductility
Energy dissipation

A B S T R A C T

This paper presents a comprehensive experimental and numerical investigation on the cyclic response of cold-formed steel columns with hollow rectangular sections. The present study examined the columns' post-buckling strength and rigidity degradation, deformation and failure modes, ductility, and energy dissipation capacity. The cold-formed steel members exhibited stable hysteretic performance up to the point of local buckling with considerable degradation in strength and ductility. The energy dissipation mechanisms from the in-plane plastic behavior and out-of-plane elastic buckling deformation were identified. The influence of the height-to-width ratio and axial-compression ratio on energy-dissipation and failure mode was also investigated.

1. Introduction

It is well-known that cold-formed thin-walled steel members with large width-to-thickness ratio are susceptible to local buckling with a post-buckling strength reserve. Over the past decades, extensive analytical, numerical, and experimental investigations on the performance of cold-formed thin-walled steel members have been reported in the literature. A summary of major research developments in cold-formed steel structures was given in Hancock [1,2]. Magnucka reviewed progresses in the field of cold-formed beams, focusing particularly on the progresses on buckling and optimal design [3]. Ellobody summarized the research works on the stability of cold-formed steel columns at ambient and fire conditions [4]. These investigations were on the static properties of cold-formed steel members, including the buckling strength, the interaction between different buckling modes, and the post-buckling load-carrying capacity of the member [5–7].

Lightweight steel structures are now increasingly being used in seismically active regions. Cold-formed steel members with hollow rectangular section may be used for critical members and components, and they are expected to undergo inelastic cyclic deformations without suffering from significant loss of strength. For thin-walled steel members, local buckling may significantly reduce the load-carrying capacity and/or ductility property of the section. On the other hand the post-buckling strength reserve may be utilized to provide the ultimate load resistance. A thorough understanding of the cyclic elastic–plastic behavior of the thin-walled steel members is fundamental to their seismic design.

During the last few decades, extensive studies have been undertaken to examine the inelastic cyclic behavior of hot-rolled steel columns, which were on the hysteretic properties under axial tension and compression load [8–10], under a combined constant axial load and cyclic bending load [11–14], or under a combined variable axial load and cyclic bending load [15]. For the hysteretic behavior of cold-formed steel members, the relevant research works focused on the bracing members, which experience the cyclic axial forces. Elchalakani described a series of tests to the failure of fix-ended cold-formed circular tubular braces under cyclic axial loading, and examined the effects of section and member slenderness on the strength, ductility, and energy absorption capacity [16]. Goggins performed quasi-static cyclic tests on bracing specimens made with cold-formed hollow steel, under idealized seismic loading conditions [17].

This paper presents a comprehensive experimental and numerical investigation on the cyclic response of cold-formed steel columns with hollow rectangular sections to assess the energy dissipation mechanism due to the coupling effect of plasticity and local buckling. Moreover, the effects of different geometric parameters on the hysteretic performances and energy-dissipation mechanism are evaluated using finite element (FE) model.

* Corresponding author. Tel.: +86 010 5168 3956; fax: +86 010 5168 7250.
E-mail address: nyang@bjtu.edu.cn (N. Yang).

http://dx.doi.org/10.1016/j.tws.2014.03.004
0263-8231/

2. Description of experimental program

2.1. Details of test specimens

A total of six cold-formed steel columns with rectangular hollow section (RHS) were tested in the present study. All specimens were made of grade Q235 steel with a nominal yield stress F_y of 235 MPa. Three cross-sectional geometries were considered, namely $160 \times 80 \times 2.49$RHS, $120 \times 80 \times 2.49$RHS, $120 \times 60 \times 2.49$RHS. Two specimen lengths (L) were considered in the cyclic tests – 1800 mm and 2300 mm. Geometric information and load control parameters of the six specimens were listed in Tables 1 and 2. Four groups of specimens were examined. Group I was comprised of R1, R2 and R3, covering different ratio of axial compression. Group II includes R3 and R5, representing different width-to-thickness ratio of web. Group III was comprised of R4 and R5, for different width-to-thickness ratio of flange. Group IV includes R4 and R9, to investigate the effect of different slenderness ratio.

The actual material characteristics of the specimens were determined from tensile coupons (dimension: $20 \times 350 \times 3$ mm^3) taken from the webs of the specimens. Table 2 summarizes the material properties. Note that the cold-forming process caused more significant increase in the yield strength for the members with larger cross-section (e.g., R1, $160 \times 80 \times 3$) than those with a smaller section (e.g., R4, $120 \times 60 \times 3$).

2.2. Test setup and loading scheme

The test setup and schematic diagram are shown in Fig. 1(a) and (b), respectively. At the ends of the member, stiffening plates were provided with adequate welding to transfer the loads. The dimension of the plates at the top and bottom ends of the specimen were $340 \times 250 \times 10$ mm^3 and $340 \times 250 \times 20$ mm^3, respectively. Two actuators placed vertically and horizontally at the top end provide combined compression and bending to the specimen. A special device called "loading head" and a horizontal beam are fixed at the top end to protect the columns from torsional deformation and out-of-plane buckling.

The ECCS loading procedure [18] is adopted as shown in Fig. 2. The load step is $0.5\delta_y$ when $\delta < \delta_y$, in which δ_y is the estimated yielding displacement evaluated from the monotonic tensile tests. The load step is switched to δ_y when the cyclic loading displacement reached δ_y, this procedure was repeated three times and the control displacement was increased until collapse of the specimen.

Table 1
Design dimensions for six tests.

Specimen	R1	R2	R3	R4	R5	R6
Height of section – H (mm)	160	160	160	120	120	120
Width of section – b (mm)	80	80	80	60	80	60
Thickness- t (mm)	2.49	2.49	2.49	2.49	2.49	2.49
Length – L (mm)	1800	1800	1800	1800	1800	2300
Slenderness ratio λ	61	61	61	82	82	105
Ratio of axial compression n	0.1	0.2	0.3	0.3	0.3	0.3

Table 2
Loading control and material parameters for six tests.

Specimen	R1	R2	R3	R4	R5	R6
Axial force N (kN)	33	66	99	73.6	82.1	73.6
Yielding displacement Δ_y (cm)	20	20	20	20	20	32
Elasticity modulus E (GPa)	240	240	240	210	189	210
Yielding stress f_y (MPa)	330	330	330	330	310	330
Ultimate stress f_t (MPa)	400	400	400	385	375	385

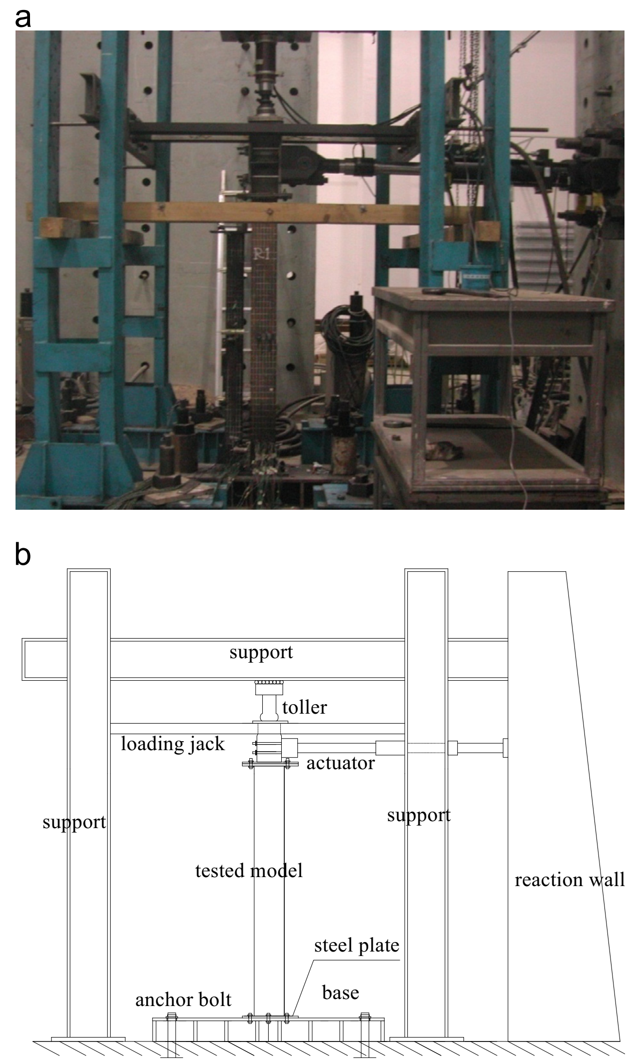

Fig. 1. Test setup (a) gernaral view of thin-walled steel members test and (b) schematic diagram of test setup.

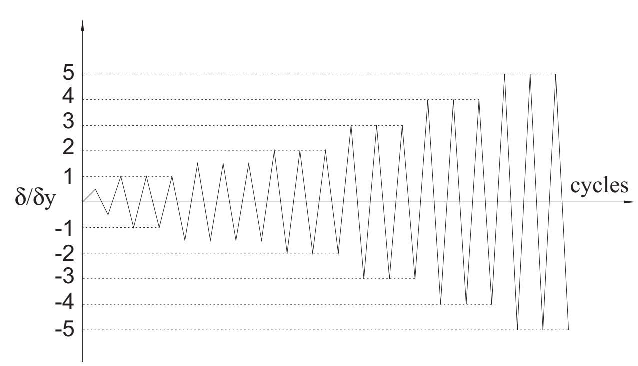

Fig. 2. ECCS loading procedures in the quasi-static test [18].

Twelve strain gauges (SG_i, $i = 1, 2, .., 12$) and four LVDT displacement transducers (DT_i, $i = 1, \ldots, 4$) were used to measure the strain and monitor the development of plasticity in the members. The arrangement of the strain gauges and displacement transducers were shown in Fig. 3. The four displacement transducers were placed: (1) on the steel plate welded at the bottom of columns to measure the relative displacement between the plate and the support (DT_1), and to observe if the bottom is slipping; (2) on the web at the bottom of the members to monitor the local buckling (DT_4); (3) at the center of the columns to record the out-of-plane